INTELLIGENT AQUACULTURE ENVIRONMENT MONITORING SYSTEM BASED ON LORA COMMUNICATION TECHNOLOGY
/
基于LoRa 通信技术的智能水产养殖环境监控系统

Huiying Cai*[1)], Fangzhen Li[1)], Peng Lv[1)], Lingqiang Ran[1)], Lida Zou[1)] [1)]
[1)] Shandong University of Finance and Economics, school of computer science and technology, Jinan / China;
Tel: +86-0531-88596229; E-mail: caihuiying323@163.com
DOI: https://doi.org/10.356.33/inmateh-63-11

Keywords: *aquaculture, monitoring system, LoRa, PLC Intelligent controller, variable universe*

ABSTRACT
*In view of the nonlinearity and large time delay characteristics of the aquaculture, this paper proposes an environment monitoring system based on low long range (LoRa) communication technology. The system integrates sensor nodes, dissolved oxygen regulation node, LoRa communication network and personal computer (PC) platform to realize real-time monitoring, storage and data sharing. The environmental parameters were processed by programmable logic controller (PLC) intelligent controller, in which, the dissolved oxygen was adjusted with the variable universe fuzzy PID algorithm. The system was tested in a fish pond with an area of 110*120 square meters. The results show that the system can obtain temperature, pH and dissolved oxygen in real time and it has the advantages of high measurement accuracy, stable and reliable data transmission, and can satisfy the needs of aquaculture intelligent management.*

摘要
*针对水产养殖非线性与大时滞的特点，本文提出了基于 LoRa 通信技术的水产养殖环境监测系统设计，系统集传感器节点、溶解氧调控节点、LoRa 通信网络、上位机平台于一体，实现了数据的实时监控、存储与共享。PLC 智能控制器对传感器采集到的环境参数进行处理并通过变论域模糊 PID 算法对水中溶解氧浓度进行智能调节。该监控系统在面积为 110*120 平方米的鱼塘进行了实验，试验结果表明：该系统可实时获取温度、pH 值、溶解氧等养殖环境参数信息系统，优势是测量精度高，数据传输稳定可靠，满足了水产养殖智能化管理的需要.*

INTRODUCTION

In recent years, the aquaculture industry of China has developed rapidly, but it still faces the problems of low efficiency and high labour intensity, and has not fully realized the intelligent management mode. The amount of aquaculture cannot meet the demand of consumption. Temperature, pH and dissolved oxygen are important water environmental parameters in aquaculture. Traditionally, the farmers obtain environmental parameters with manual sampling and chemical analysis which is time-consuming and the accuracy of the parameters is low.

The rapid development of Internet of things technology has played an important role in changing the current extensive breeding mode. Researchers have carried out a variety of related research work and achieved important results. The android platform aquaculture remote monitoring system based on the Internet of things was designed to realize the remote monitoring of water quality sensor parameters with good real-time performance (*Sang Q.S., 2018*).

Through the integration of internet of things and GIS technology, a centralized management of regional aquaculture management was proposed and can promote the development of aquaculture to the direction of intelligence and information (*Zhao R.Y., 2020*).

A smart data gathering system for monitoring several parameters in aquaculture tanks was designed using a wireless sensor network (*Parra L., Sendra S., 2017*).

A low-cost water-quality monitoring system based on ZigBee is reported to measure the important variables in precision aquaculture (*López R.A.B., Cordova L.R.M. et al, 2020*). This paper puts forward an aquaculture environment monitoring system based on LoRa communication technology which is a popular communication protocol of Internet of things technology.

[1] *Huiying Cai, Ph.D.; Fangzhen Li, Ph.D.; Peng Lv, Ph.D.; Lingqiang Ran, Ph.D.; Lida Zou, Ph.D.;*

The system, which is composed of hardware part and upper computer platform, realizes the remote collection function of aquaculture environmental parameters (pH, temperature, dissolved oxygen) and the regulation function of dissolved oxygen in water. The hardware part is composed of sensor node, dissolved oxygen regulation node and LoRa communication network. The sensor node uses ARM cortex m3 core based stm32f103c8t6 processor to collect breeding environment information and upload gateway free data through LoRa communication module. LoRa communication protocol has the advantages of low power consumption, long communication distance, automatic frequency hopping and rate adaptive function. The dissolved oxygen regulation node adopts Siemens smart controller to control the on-site aerator and feeding equipment. The PC platform can monitor the signal strength of the sensor node LoRa antenna, which provides a basis for on-site layout of sensor nodes and the evaluation of the quality of communication links.

MATERIALS AND METHODS

System architecture

The parameters detected by the aquaculture environment monitoring system include temperature, dissolved oxygen and pH. The architecture of the monitoring system is shown in Figure 1. It consists of the physical layer, communication layer and application layer. The physical layer is used to collect breeding environment parameters and receive control signals to control dissolved oxygen concentration. The circuits to collect the temperature, dissolved oxygen and pH are designed on the stm32f103c8t6 based sensor nodes of the physical layer. The dissolved oxygen concentration and the feeding equipment are controlled through the digital quantity interface by the PLC controller. LoRa communication module with RS485 interface is equipped between PLC controller and server of host computer to receive data command. The communication layer is used to transmit breeding environment information and dissolved oxygen regulation information. The application layer is used to query, storage and share data.

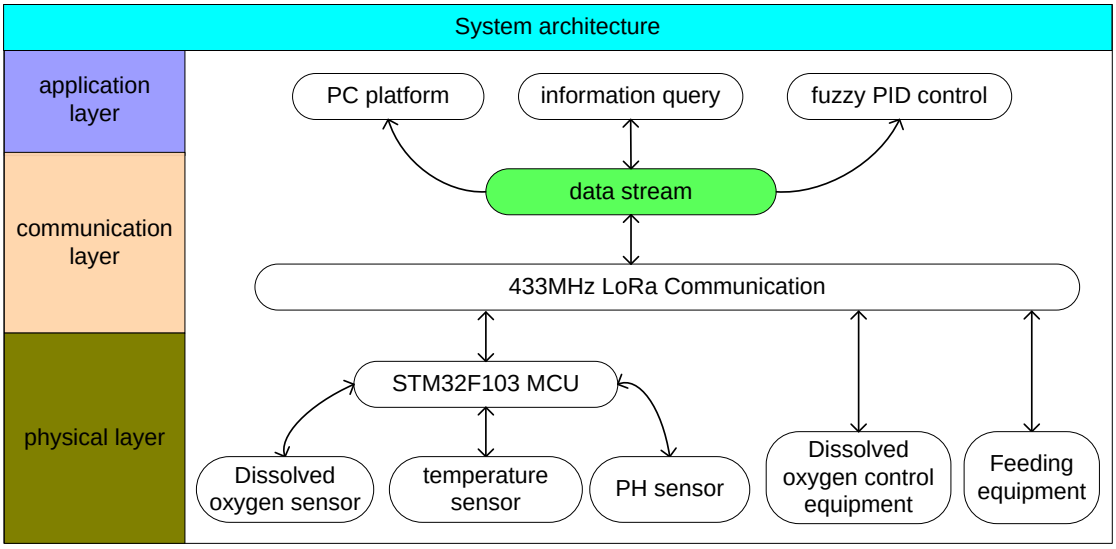

Fig.1 - System framework

Design of the sensor nodes

Hardware structure design of wireless sensor network node

The hardware structure design of sensor network node is shown in Figure 2. The sensor network node includes the temperature sensor, dissolved oxygen sensor, pH sensor, A/D conversation circuit, processor, LoRa module and flash memory. The wireless sensor network node is powered by solar cells which are widely used in the control system of agriculture (*Ravishankar E., Booth R.E. et al, 2020*) and aquaculture (*El-Atab N., Almansour R., 2020*).

The core processor is ARM cortex m3 core based stm32f103c8t6 which has Serial Peripheral Interface (SPI) interface and A/D conversation interface to acquire, analyse, store and upload data. LoRa module and flash memory communicate with processor through the SPI interface. Temperature, dissolved oxygen and pH are acquired by the temperature sensor, dissolved oxygen sensor and pH sensor respectively. The sensors are processed by the information analysis module and connected with the A/D interface of the processor.

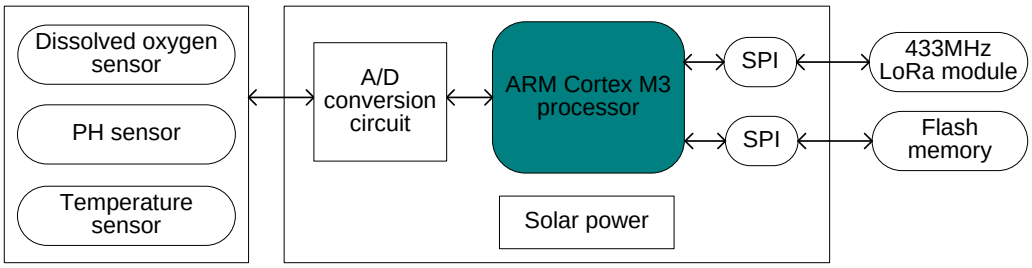

Fig.2 – Design of sensor network node

The hardware circuit of sensor network node is shown in Figure 3. Figure 3a is the power supply module which adopts 12V power supply. The power interface is protected by high reliability devices. The first level protection adopts varistor 14d470k (MOV1), 1.1A/60V fuse (FUSE1), transient voltage suppressor (TVS) SMCJ36CA (D4). The varistor 14d470k whose action voltage is 47 V and peak current is 1 KA (8/20us pulse) can absorb strong energy interference. The response speed of TVS SMCJ36CA is fast. Benefit from these components, the first level protection is used to absorb large current and voltage generated by electromagnetic interference. The second level protection includes TVS SMCJ36CA (D60), common mode inductor acp3225-102 and ceramic air discharge tube smd1812-151 (D50) group. In the case that the primary protection fails or cannot absorb interference completely, the secondary protection will play a significant role in absorbing interference. The asynchronous buck power chip mp1482 converts the input 12-18 V into 3.3 V for sensor nodes, and can provide 2A load current. In this power supply system, the anti-power supply surge differential mode interference can reach 1 KV voltage while anti-common mode interference can reach 1 KV voltage.

The main control module stm32f103c8t6 interacts with LoRa communication module through SPI communication interface. LoRa communication module uses lsd4rf-2r717n10 of which working frequency band is 860-935 MHz. It adopts LoRa modulation mode and is compatible with and supports 2FSK and GFSK traditional modulation mode. Hardware frequency hopping technology is combined with LoRa spread spectrum technology, which can achieve better communication concealment and security. W25x16 is selected as the flash memory of which the storage space is 16 MB**,** the communication rate can reach 72 MHz, and the current consumption is 0.5 mA under normal working condition. The memory communicates with stm32f103c8t6 through SPI interface.

The dissolved oxygen acquisition circuit is shown in Figure 3b. It uses the polarographic film dissolved oxygen electrode composed of platinum electrode and silver electrode. Dissolved oxygen electrode generates current type signal when 0.7 V excitation voltage is applied to platinum electrode and silver electrode. In the circuit, two-stage operational amplifier circuits (U1, U2) with ±3.3 V power supply are used to process the current signal. U1 converts the current generated by dissolved oxygen electrode into voltage through resistance R1, and U2 further filters and amplifies the voltage. The calculation formula of dissolved oxygen voltage is shown in Equation (1), in which, V_{ab}, I, R_1, R_2, R_6 represents the dissolved oxygen voltage, the output current of the dissolved oxygen electrode, and the fixed resistances respectively.

$$V_{do} = \frac{R_1 R_2}{R_6} I \tag{1}$$

The pH acquisition circuit is shown in Figure 3c. It uses a composite electrode composed of calomel electrode and glass electrode to measure pH. When the concentration of hydrogen ion changes, the electromotive force between calomel electrode and glass electrode will change, and the weak voltage signal will be output. This module uses two-stage operational amplifier circuits (U3, U4) with ±3.3 V power supply. U3 is a reverse amplifying circuit, and the voltage magnification is adjusted by sliding resistance. U4 reverses the output voltage signal of U3 to meet the input range of 0-3.3 V. The resistors R3 and R4 can adjust the reference of adjustable output voltage signal. The power filter capacitor C4, C5, C6, and C7 can filter out the high-frequency interference and make the power supply stable. The voltage signal of pH can be calculated by Equation (2), in which, V_{ph} is the voltage signal of pH and R_1, R_2, R_3, R_4, R_5, R_6, R_8 are resistors with fixed value.

$$V_{ph} = \frac{3.3R_3}{R_3 + R_4}\left(1 + \frac{R_8}{R_6}\right) - \frac{R_8}{R_6}\left(1 + \frac{R_1 + R_2}{R_5}\right) \tag{2}$$

Temperature acquisition circuit is shown in Figure 3d. The bridge circuit is composed of R1, R2, R3, and R4, in which, R4 is the built-in thermistor (NTC-MF52AT). U5A, U5B is the two stage operational amplifier to amplify the voltage signal. U5A is a differential operational amplifier which can effectively amplify the differential mode voltage and suppress the common mode voltage. U5B can further process the voltage signal processed by U5A to make it fall in the A/D converter range. PR1 and PR2 can adjust the output reference voltage and output magnification voltage respectively. The collected temperature signal can be computed by Equation (3), in which, V_t is the voltage of the temperature signal and the other symbols with R as superscript are resistors with fixed value.

$$V_t = \frac{3.3R_{PR1}}{R_{16}+R_{PR1}}\left(1+\frac{R_{PR2}}{R_6}\right)-\frac{R_{PR2}}{R_6}\left(\frac{3.3R_3R_7(R_{11}+R_{12})}{R_{11}(R_2+R_3)(R_7+R_8)}-\frac{R_4R_{12}}{R_{11}(R_1+R_4)}\right) \quad (3)$$

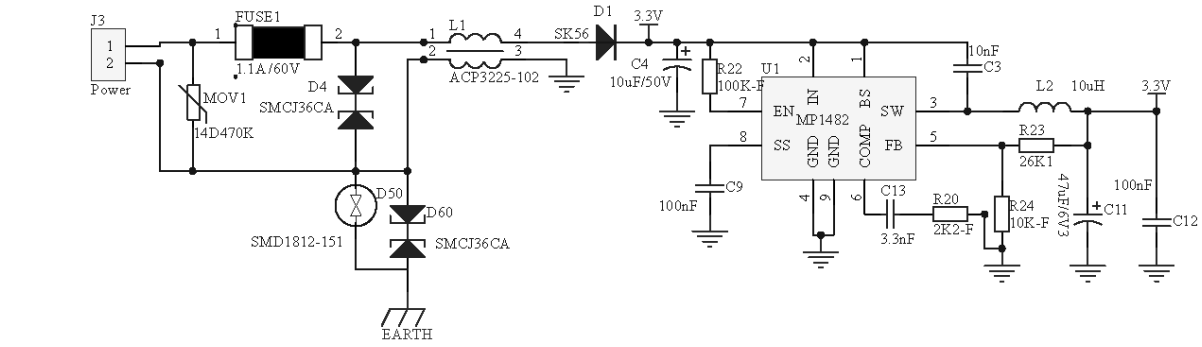

(a) power supply circuit

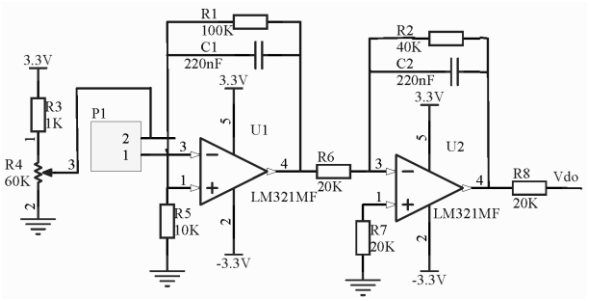

(b) Dissolved oxygen acquisition circuit

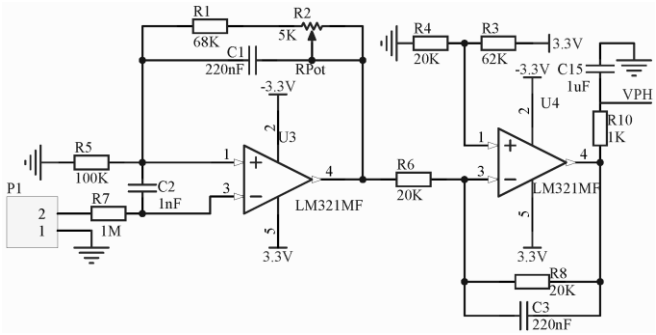

(c) pH acquisition circuit

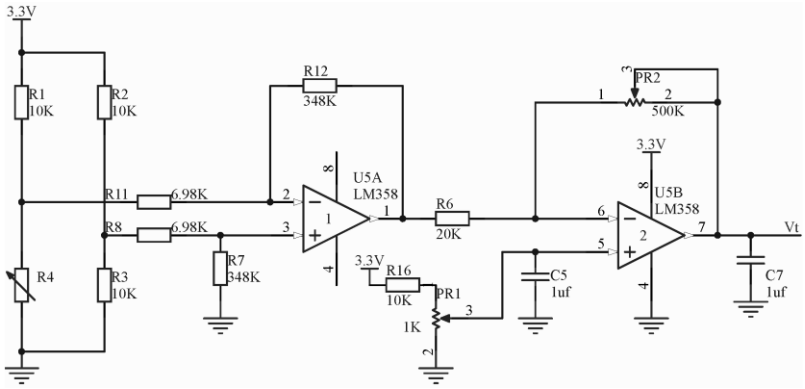

(d)Temperature acquisition circuit

Fig. 3 – Hardware design of sensor nodes

Software design of wireless sensor network node

The software of sensor network node is based on the embedded UC/OS-II operation system which has the advantages of preemptive, multi task and real-time (*Ungurean, I., 2020*). It can create 64 tasks. The tasks, priority, stack size and function established in the monitoring system are listed in table 1. The sensor network nodes are powered and the operation system and outside devices are initialized firstly. Then the task control function establishes the temperature, pH, dissolved oxygen, LED flashing, upload communication tasks, and assign priority and stack space to them. Sensor network node uses CRC verification and can transmit, receive, and converse data.

Table 1

The tasks of the operating system

Task	Priority	Stack size (K)	Function
WenDuTaskTCB	5	512	read temperature
PHTaskTCB	6	512	read pH
RongJieYangTaskTCB	7	512	read dissolved oxygen
LEDTaskTCB	9	128	LED flashing indication
TongXinTaskTCB	4	1024	communication

Calibration of sensors

As temperature, dissolved oxygen, and pH are represented through voltage which is susceptible to temperature, it is necessary to calibrate the relationship between output voltage and temperature of each sensor. Different solutions are put into the constant temperature magnetic stirrer. It was cooled into 1℃. And then the temperature was increase by 1℃ every 10 minutes. Fifty values were acquired during this process. Each value was sampled ten times by the corresponding modules and the average value was used.

The correlation coefficient of the output voltage and temperature was computed. The dissolved oxygen sensor and pH sensor use saturated sodium sulphite solution and standard solution with pH = 7 respectively.

The calibration curves are shown in Figure 4. Figure 4a and figure 4b show linear relationship between the independent variable and dependent variable of dissolved oxygen and pH. The correlation coefficient of dissolved oxygen sensor and pH sensor are 0.994 and 0.9969 respectively.

Figure 4c shows that there is an inflection point in the fitted curve where the slope of the curve is the largest. In the range of [1, 25] and [25, 50], there is a piecewise linear relationship respectively, and the correlation is strong. The linear correlation function is shown in Figure 4c.

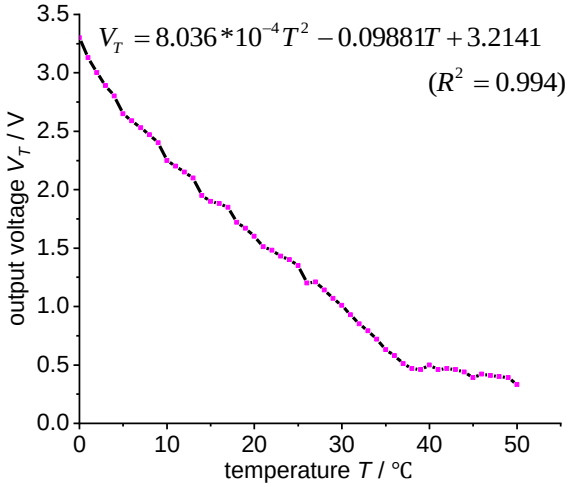

(a) The relationship between voltage and temperature of dissolved oxygen

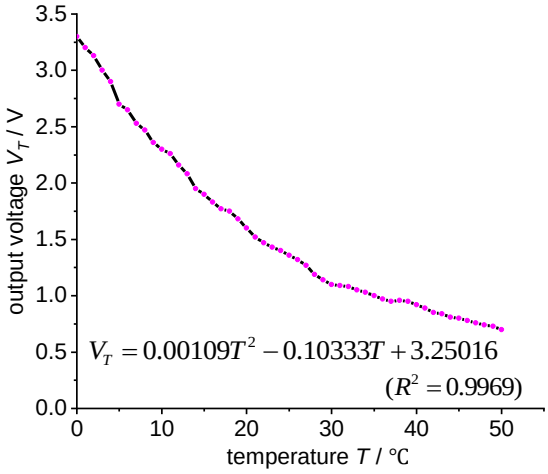

(b) The relationship between voltage and temperature of pH

Fig. 4 - Calibration curves

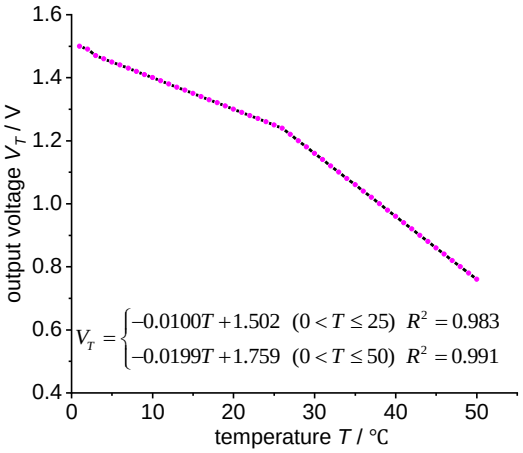

(c) The relationship between voltage and temperature

Fig. 4 c - Calibration curves

Design of the dissolved oxygen regulation equipment

The dissolved oxygen regulation equipment adopts Siemens PLC controller S7-200 which is equipped with RS485 communication interface and supports Modbus RTU, USS and free port communication protocol (*Liu T., Zhao K. et al, 2020*). The system structure of dissolved oxygen regulation equipment is shown in Figure 5. The dissolved oxygen regulation equipment adopts 380 V three-phase AC motor (M1), and the feeding equipment adopts 220 V AC motor (M2). QS1 and QS2 are power switch circuit breakers, FU1 and FU2 are fuses, KM1 and KM2 are AC contactors, FR1 and FR2 are thermal relays. The output ports Y0 and Y1 control the dissolved oxygen regulation equipment and the feeding equipment respectively. LoRa communication equipment and PLC controller are connected through RS485 interface. In the automatic control mode, QS1 and QS2 are closed. When the LoRa communication equipment receives the command to open the dissolved oxygen regulation equipment or feeding equipment, the information is transmitted to the PLC controller through RS485 interface. The corresponding output ports Y0/Y1 of PLC acts, and the coil KM1/KM2 is powered on. Then, the main contact KM4/KM3 is closed, and the motor M1/M2 rotates. KM4/KM3 is used as the auxiliary contact of AC contactor to judge the closed state of contactor.

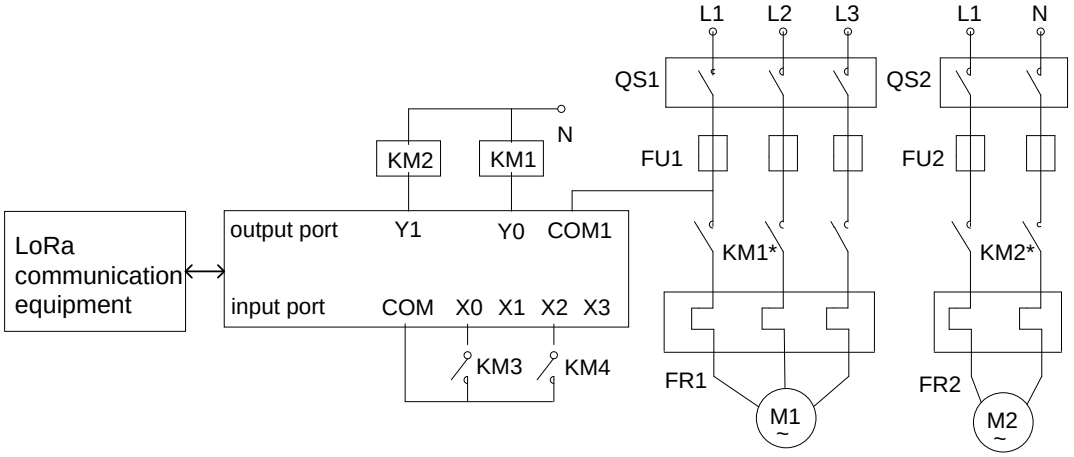

Fig. 5 - Schematic diagram of dissolved oxygen regulation equipment

Communication design

Data transmission of communication layer depends on wireless communication module lsd4rf-2r717n10 with 433MHz. The main chip is SX1278 which can adjust the transmission power. The sensor node adopts monitoring mode and is in sleep mode when there is no data acquisition command.

The PC software platform will measure the RSSI value of each communication to evaluate the link communication quality. The RSSI value can be used to optimize the deployment of field nodes. Unreliable communication will happen as occasionally as there are co frequency interference and plant occlusion in the complex outdoor environment. In this case, the platform sets the RSSI value according to the actual needs to make it in the right range. And the platform will issue the corresponding command to adjust the node

transmission power to ensure the best communication quality. The transmission distance between sensor node and platform terminal and the relationship between receiving power and transmitting power are computed according to Equation (4).

$$P_R = P_T / r^n \tag{4}$$

In which, P_R, P_r, r, n represents wireless signal receiving power, wireless signal transmitting power, transmission distance and propagation factor, respectively.

The other form of Equation (4) can be expressed as Equation (5). Equation (5) shows that the received power changes in an inverse exponential curve.

$$P_R = B - 10 \cdot n \cdot \lg(r) \tag{5}$$

Remote monitoring terminal

Communication between sensor network nodes and host computer

There are two ways to upload the data: the node actively reports the data and the software platform queries the data. The data is communicated through LoRa. If the upload is successful, the sensor network nodes will sleep in the low-power mode after feedback. When the software platform queries the pH, the command denoted by 09 02 00 00 00 02 F8 8C is send. In the command, 09 represent device address, 02 represents function code, 00 00 and 00 02 represents starting address of the register and the number of bytes to read respectively, F8 8C represents the CRC verification. The returned data frame is 09 03 04 XX XX 00 02 22 74. In the frame, the first, second and third bytes represent the device address, function code and the total number of bytes of returned pH respectively, the fourth and fifth bytes are pH, the sixth and seventh bytes represent decimal places, and the eighth and ninth bytes represent CRC verification. XX XX represents the value of pH in hexadecimal system. 00 02 represents that pH has two decimal places. For example, 03 09 can be converted into decimal number 1411 and the value of pH is 14.11.

In order to improve the efficiency of communication, the temperature information is uploaded together with the data of dissolved oxygen. When the software platform queries the dissolved oxygen and temperature values, it sends the command: 03 03 00 00 00 04 45 EB, in which, the first 03 is the device address, the second 03 is the function code, 00 00 is the starting address of the register, 00 04 is the number of bytes to read, and 45 EB is the CRC check. The returned data is: 03 02 08 XX XX 00 02 YY YY 00 01 5C 45, in which, 03, 02, and 08 represent device address, function code, and number of returned bytes respectively. XX XX represents the value of dissolved oxygen. 00 02 denote the number of decimal places. YY YY is the value of temperature. 00 01 denote the number of decimal places. 5C 45 is the CRC verification.

Dissolved oxygen regulation

Variable universe fuzzy control has shown significant potential in real-time control (*Yang S.M., Deng B. et al, 2019*). So, it is adopted to solve the large time delay problem of dissolved oxygen in pond. The control diagram is shown in Figure 6. The dissolved oxygen sensor sends the collected data to the PLC controller through LoRa communication protocol, and the PLC controls the aerator according to the variable universe fuzzy PID control algorithm.

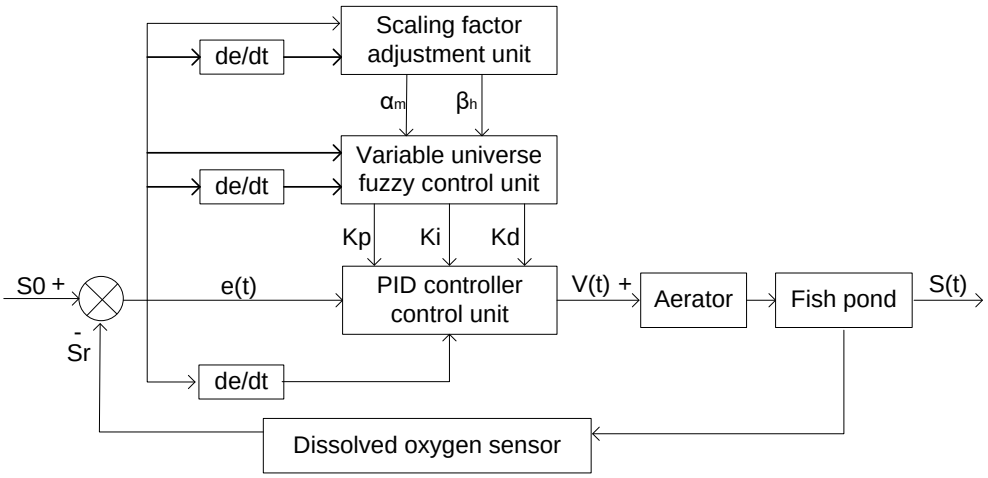

Fig. 6 - Diagram of the variable universe fuzzy control

Fuzzy PID control algorithm

The fuzzy PID algorithm (*Ren Q., 2020*) is adopted to adjust the dissolved oxygen. The fuzzy subsets of input variables e, ec and out variables $\triangle K_P$, $\triangle K_I$, $\triangle K_D$ are {NB, NM, NS, ZO, PS, PM, PB}, representing negative big, negative middle, negative small, zero, positive small, positive middle, positive big, respectively. The basic domains of e, ec, $\triangle K_P$, $\triangle K_I$, $\triangle K_D$ are [-9, 9], [-2, 2], [-10, 10], [-0.5, 0.5], [-10, 10], respectively. The fuzzy domains of input and output are {-6, -5, -4, -3, -2, -1, 0, 1, 2, 3, 4, 5, 6}. The quantification factors of e, ec, $\triangle K_P$, $\triangle K_I$, $\triangle K_D$ are K_e=6/9=0.67, K_{ec}=6/2=3, K_{rP}=10/6=1.67, K_{rI} =0.5/6=0.083, K_{rD}=10/6=1.67, respectively.

Membership function is an important factor to determine the control effect of fuzzy controller (*Mani P., Rajan R. et al, 2021*). In order to better restrain the change of dissolved oxygen, this paper uses trapezoidal function as the input and output membership function of fuzzy controller, as shown in Equation (6), in which, F_{trapmf} is the membership value, x is the universe value of fuzzy controller, and a, b, c, d is the parameter of trapezoidal membership function.

$$F_{trapmf} = \begin{cases} 1 & (c \le x \le b) \\ \dfrac{a-x}{a-b} & (b \le x \le a) \\ \dfrac{c-x}{c-d} & (d \le x \le c) \\ 0 & (a \ge x \ or \ x \le d) \end{cases} \tag{6}$$

Based on the experience of breeding operators and the technical knowledge of dissolved oxygen regulation design experts, a fuzzy control unit with two-dimensional input (e, ec) and three-dimensional output ($\triangle K_P$, $\triangle K_I$, $\triangle K_D$) is constructed. The fuzzy rules of the fuzzy control unit are shown in Table 2.

Table 2

Adjusting rules of KP/KI/KD for fuzzy PID controller

$\triangle K_P$ /$\triangle K_I$ /$\triangle K_D$		error variation: e						
		NB	NM	NS	ZO	PS	PM	PB
ec	NB	PB/NB/PS	PM/NB/ZO	PM/NM/ZO	PM/NM/ZO	PS/NS/ZO	PS/ZO/PB	ZO/ZO/PB
	NM	PM/NB/NS	PM/NM/NS	PM/NM/NS	PM/NS/ZO	PS/NS/ZO	ZO/ZO/NS	ZO/ZO/PM
	NS	PM/NM/NB	PM/NM/NB	PS/NS/NM	PS/NS/NS	ZOZO/ZO	ZO/ZO/ZO	NS/PS/PM
	ZO	PM/NS/NB	PS/NS/NM	PS/NS/NM	ZO/ZO/NS	NS/ZO/ZO	NS/PS/PS	NS/PS/PM
	PS	PS/NS/NB	PS/NS/NM	ZO/ZO/NS	NS/PS/NS	NS/PS/ZO	NM/PM/PS	NM/PM/PM
	PM	ZO/ZO/NM	ZO/ZO/NS	NS/PS/NS	NM/PS/NS	NM/PM/ZO	NM/PM/PS	NM/PB/PS
	PB	ZO/ZO/PS	NS/ZO/ZO	NS/PS/ZO	NM/PM/ZO	NM/PM/ZO	NM/PB/PS	NB/PB/PM

Variable universe scaling factor adjustment unit

In fuzzy PID control, the scope of universe is not changed, which cannot solve the problem of low control accuracy and affect the overall performance of the control system. Based on Fuzzy PID control, a variable universe adaptive fuzzy PID controller is designed, which can effectively solve the problem of low control accuracy and overshoot. After the expansion of variable universe, the scope of universe is shown in Equation (7), in which, α_m, β_h, denotes the expansion factors of input and output universe respectively. The scope of universe $E(e_1)$, $E(e_2)$ decreases with the decrease of deviation and expands with the increase of deviation. For the nonlinear dissolved oxygen system, the time-varying error is effectively suppressed and the control accuracy is improved.

$$\begin{cases} E(e_1) = \left[-\alpha_e(e_1)\times 9, \alpha_e(e_1)\times 9\right] \\ E(e_2) = \left[-\alpha_{ec}(e_2)\times 2, \alpha_{ec}(e_2)\times 2\right] \\ U(e_1,e_2) = \left[-\beta(e_1,e_2)u_1, \beta(e_1,e_2)u_2\right] \end{cases} \tag{7}$$

The variable universe expansion factor must satisfy the duality and coordination in the design. In this paper, the proportional expansion factor based on function design is adopted.

It is shown in Equation (8), where, λ is the proportional constant $\lambda \in (0, 1)$, $\beta(0)$ is the initial value, k_m is the design parameter.

$$\begin{cases} \alpha_m(x) = 1 - \lambda \exp(-k_m x^2) & (m = e, ec) \\ \beta_h(y) = K \sum_{i=1}^{n} p_i \int_0^t e_i(\tau) d\tau + \beta(0) & (n = p, i, d) \end{cases} \quad (8)$$

According to the characteristics of dissolved oxygen regulation combined with practical work experience, the input and output expansion factors are taken respectively, as shown in Equation (9).

$$\begin{cases} \alpha_1(e) = 1 - 0.61\exp(-0.55e^2) \\ \alpha_2(ec) = 1 - 0.61\exp(-0.63ec^2) \\ \beta_p = 3.5|e| \\ \beta_i = \dfrac{1}{|e| + 0.55} \\ \beta_d = 4.2|e| \end{cases} \quad (9)$$

RESULTS

The experiments of LoRa communication, acquisition of water quality parameter data and dissolved oxygen regulation were conducted in a fish pond whose area is 110*120 square meters. The LoRa communication experiment is used to verify the stability and reliability of LoRa communication network transmission. The data acquisition experiment is used to verify the accuracy of parameter acquisition and the correctness of transmission. The dissolved oxygen regulation experiment is to verify the control accuracy of dissolved oxygen content in fish ponds.

LoRa communication experiment

In order to test the performance of LoRa communication module, the communication experiment was carried out in the open environment and the occluded environment. The occluded environment refers to the environment with tree sheltered or telegraph poles or something that blocks the signal. The results are shown in Fig 7.

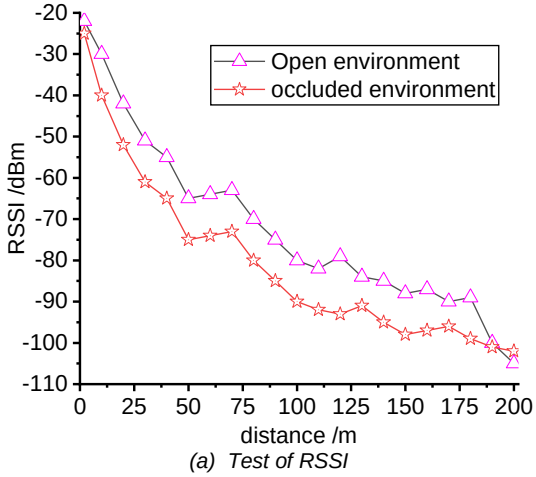

(a) Test of RSSI

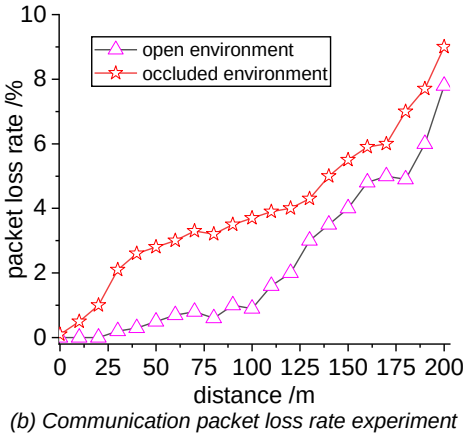

(b) Communication packet loss rate experiment

Fig. 7 – Communication performance experiment of LoRa

Figure 7a shows the performance of LoRa RSSI. In the open environment, when the transmission distance varies from 0 meter to 25 meters, RSSI changes slowly and decreases from – 24 dBm to – 60 dBm gradually. RSSI decreases to -100 dBm when the transmitting and receiving distance reaches 170 meters. In the occluded environment, RSSI will also decrease with the increase of communication distance. Compared with the open environment, the RSSI will be lower at the same distance. The experimental results are consistent with the theoretical relationship that the intensity of LoRa signal changes with the increase of transmission distance.

Figure 7b shows the result of communication packet loss rate experiment. In the open environment, the packet loss rate is higher than 4% when the transmission distance exceeds 150 meters and the RSSI value is – 95 dBm. The packet loss rate increases with the further increase of distance. The packet loss rate reaches 8% when the communication distance is 200 meters and RSSI value is – 105 dBm. Compared with the open environment, the overall change trend of packet loss rate in the occluded environment is slower. The packet loss rate reaches 9% when the transmission distance is 200 meters.

Therefore, an open environment should be chosen and the distance should be controlled within 100 meters to get better signal strength and lower packet loss rate.

Data acquisition experiment

In order to verify the accuracy of aquatic parameter, the data of sensor network nodes were collected in different weather (sunny, cloudy, light rain), different time periods (8:30, 12:00, 19:30). The parameters measured by hash MS5 Hydrolab water quality monitor were taken as the standard values. The results are shown in table 3, from which, it can be seen that: the temperature acquisition accuracy is less than or equal to 0.15, the average relative error is 0.1%; the dissolved oxygen acquisition accuracy is less than or equal to 0.29, the average relative error is 0.8%; the pH value acquisition accuracy is less than or equal to 0.17, the average relative error is 0.81%.

Table 3

Results of Data acquisition experiment

Date	Parameter	Time	Standard value	Actual value	Relative error (%)
September 20, 2020 (sunny)	Temperature (℃)	8: 00	26.86	26.84	-0.07
		12: 00	27.82	27.80	-0.07
		19: 30	27.32	27.35	0.12
	Dissolved oxygen (mg/L)	8: 30	4.62	4.91	6.2
		12: 00	7.60	7.64	0.53
		19: 30	5.72	5.63	-1.57
	pH	8: 30	8.32	8.32	0
		12: 00	6.89	6.92	0.44
		19: 30	8.32	8.33	0.12
September 22, 2020 (cloudy)	Temperature (℃)	8: 30	25.12	25.11	-0.04
		12: 00	25.02	25.13	0.44
		19: 30	24.98	24.96	-0.08
	Dissolved oxygen (mg/L)	8: 30	4.97	5.08	2.21
		12: 00	8.21	8.06	-1.83
		19: 30	4.72	4.88	3.39
	pH	8: 30	6.98	7.12	2.01
		12: 00	6.62	6.72	1.51
		19: 30	7.02	6.98	-0.57
September 24, 2020 (light rain)	Temperature (℃)	8: 30	25.12	25.11	-0.04
		12: 00	26.56	26.58	0.08
		19: 30	25.61	25.46	0.58
	Dissolved oxygen (mg/L)	8: 30	4.89	4.68	-4.29
		12: 00	6.12	6.27	2.45
		19: 30	5.88	5.89	0.17
	pH	8: 30	8.35	8.47	1.44
		12: 00	7.18	7.20	0.28
		19: 30	7.98	8.15	2.13

Dissolved oxygen experiment

In order to verify the regulation accuracy of field control equipment for dissolved oxygen in pond, the regulation test was conducted in pond. Four node sensors, whose average value was taken as the dissolved oxygen amount, were placed in the four corners of the pond. 5 KW impeller aerator is placed in the centre of the pond. The control target value of dissolved oxygen is set to be 7.1 mg/L. In order to verify the control effect of variable universe fuzzy PID controller of dissolved oxygen, self-organizing fuzzy neural controller and fuzzy PID controller are used for comparison. The software platform is set to collect data every 30 minutes, and the collection time is 24 hours. Figure 8 shows the data curve of dissolved oxygen regulated by three controllers. The fluctuation of variable universe fuzzy PID controller is the minimum after the regulation becomes stable. Table 3 shows the comparison data of the performance of the three controllers. From the table, it can be seen that each index of the variable universe fuzzy PID controller has obvious advantages: the regulation time is 53 minutes; the minimum overshoot is 4.89%; the standard deviation is 0.056; and the average error is 0.2. The variable universe fuzzy PID controller has the best performance.

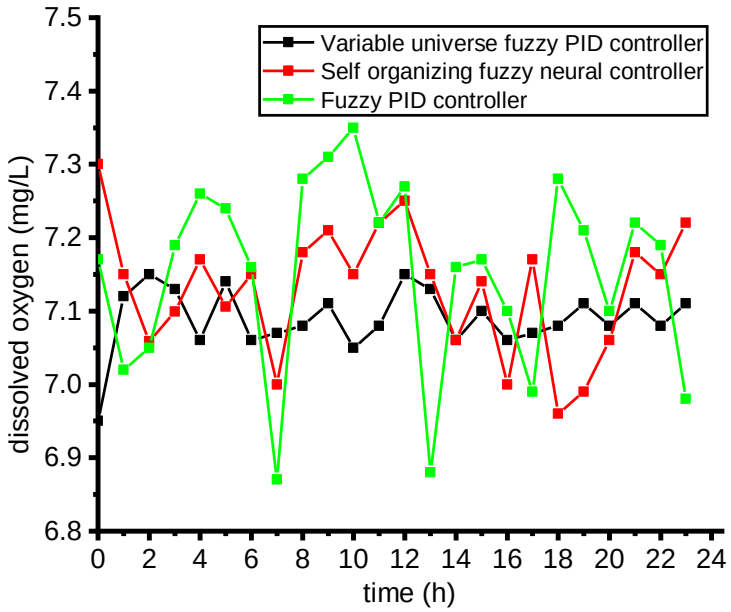

Fig. 8 - Performance test of dissolved oxygen regulation

Table 4

Comparison of controller performance parameters

Parameter	Variable universe fuzzy PID control	Self-organizing fuzzy neural controller	Fuzzy PID control
Adjustment time /min	53	80	120
Overshoot /%	4.89	8.25	16.49
Standard deviation	0.056	0.125	0.223
Average error	0.02	0.05	0.10

CONCLUSIONS

According to the characteristics of aquaculture environment, this paper designed an aquaculture environment monitoring system which integrates advanced technologies LoRa communication technology, variable universe fuzzy PID control and PLC control technology. The system realized the accurate measurement of water quality parameters (temperature, dissolved oxygen, pH) in aquaculture environment and the regulation of dissolved oxygen in water. It can effectively restrain the disturbance caused by uncertain factors in aquaculture environment and has high steady-state precision and strong regulation ability.

ACKNOWLEDGEMENT

This work was financially supported by the Department of Education of Shandong Province, grant no. KJ2018BAN058.

REFERENCES

[1] EI-Atab N., Almansour R. et al., (2020), Heterogeneous cubic multidimensional integrated circuit for water and food security in fish farming ponds, *Small*, vol. 16, no. 4, article number: 1905399, Weinheim/Germany (DOI: 10.1002/smll.201905399);

[2] Liu T.R., Zhao K., Sun C.L. et al., (2020), Real-time flow control of blade section using a hydraulic transmission system based on an H-Inf controller with LMI design, *Energies*, vol. 13, no. 19, article number: 5029, Basel/Switzerland (DOI: 10.3390/en13195029);

[3] Lopez R.A.B., Cordova L.R.M., Nunez J.C.G. et al., (2020), Implementation and evaluation of open-source hardware to monitor water quality in precision aquaculture, *Sensors*, vol. 20, no. 21, article number: 6337, Basel/Switzerland (DOI: 10.3390/s20216112);

[4] Mani P., Rajan R., Joo Y.H., (2021), Integral sliding mode control for T-S fuzzy descriptor systems, *Nonlinear Analysis Hybrid Systems*, vol. 39, article number: 100953, Netherlands (DOI: 10.1016/j.nahs.2020.100953);

[5] Parra L., Sendra S., Llore J., Rodrigue, J.J.P.C., (2017), Design and deployment of a smart system for data gathering in aquaculture tanks using wireless sensor networks, *International Journal of Communication Systems*, vol. 30, no. 16, article number: e3335, Chichester/England (DOI: 10.1002/dac.3335);

[6] Ravishankar E., Booth R.E., Saravitz C. et al., (2020). Achieving net zero energy greenhouses by integrating semitransparent organic solar cells, *Joule*, vol. 4, no. 2, pp. 490-506, Cambridge/USA;

[7] Ren Q., (2020), Intelligent control technology of agricultural greenhouse operation robot based on Fuzzy PID path tracking algorithm, *INMATEH Agricultural Engineering*, vol. 62, no. 3, pp. 181-190. Bucharest/ Romania;

[8] Sang Q.S., (2018), *Aquaculture remote monitoring system based on Internet of things and mobile terminal (基于物联网和移动终端的水产养殖远程监控系统)*, MSc dissertation, Wuhan Institute of Technology, Wuhan/China;

[9] Ungurean I., (2020), Timing comparison of the real-time operating systems for small microcontrollers, *Symmetry-Basel*, vol. 12, no. 4, article number: 592, Basel/Switzerland (DOI: 10.3390/sym12040592);

[10] Yang S., Deng B., Wang J. et al., (2019), Design of hidden-property-based variable universe fuzzy control for movement disorders and its efficient reconfigurable implementation, *IEEE Transactions on Fuzzy Systems*, vol. 27, no. 2, pp. 304-318, NJ/USA;

[11] Zhao R.Y., (2020), Design of remote monitoring system for aquaculture boat based on SuperMap GIS and Android platform *(基于超图GIS 和Android 平台的水产养殖船远程监控系统设计)*, MSc dissertation, Jiangsu University, Jiangsu/China.